Check for updates

Meteoritics & Planetary Science 58, Nr 9, 1365–1381 (2023)
doi: 10.1111/maps.14041

Report

Bulk mineralogy, water abundance, and hydrogen isotope composition of unequilibrated ordinary chondrites

Helen GRANT[1]*, Romain TARTÈSE[1], Rhian JONES[1], Laurette PIANI[2], Yves MARROCCHI[2], Ashley KING[3], and Thomas RIGAUDIER[2]

[1]Department of Earth and Environmental Sciences, The University of Manchester, Manchester, UK
[2]CNRS, CRPG, UMR 7358, Université de Lorraine, Vandoeuvre les Nancy, France
[3]Planetary Materials Group, Natural History Museum, London, UK
***Correspondence**
Helen Grant, Department of Earth and Environmental Sciences, The University of Manchester, Manchester M13 9PL, UK.
Email: helen.grant@manchester.ac.uk

(Received 04 April 2023; revision accepted 12 June 2023)

Abstract–The origin and transport of water in the early Solar System is an important topic in both astrophysics and planetary science, with applications to protosolar disk evolution, planetary formation, and astrobiology. Of particular interest for understanding primordial water transport are the unequilibrated ordinary chondrites (UOCs), which have been affected by very limited alteration since their formation. Using X-ray diffraction and isotope ratio mass spectrometry, we determined the bulk mineralogy, H_2O content, and D/H ratios of 21 UOCs spanning from petrologic subtypes 3.00–3.9. The studied UOC falls of the lowest subtypes contain approximately 1 wt% H_2O, and water abundance globally decreases with increasing thermal metamorphism. In addition, UOC falls of the lowest subtypes have elevated D/H ratios as high as those determined for some outer Solar System comets. This does not easily fit with existing models of water in the protoplanetary disk, which suggest D/H ratios were low in the warm inner Solar System and increased radially. These new analyses confirm that OC parent bodies accreted a D-rich component, possibly originating from either the outer protosolar nebula or from injection of molecular cloud streamers. The sharp decrease of D/H ratios with increasing metamorphism suggests that the phase(s) hosting this D-rich component is readily destroyed through thermal alteration.

INTRODUCTION

The hydrogen (H) isotope composition of water, given by its D/H ratio, is one of the key proxies to understand its origin(s) and processing in the early Solar System (e.g., Broadley et al., 2022; Ceccarelli et al., 2014; Hallis, 2017; Robert, 2006). Because deuterium (D) is twice as heavy as ^{1}H, physical and (bio)chemical processes can induce large fractionations of D to H ratios, making it an ideal isotopic tracer. For example, within the Solar System, D/H ratios vary from ~20 × 10^{-6} for H_2 from the Sun and the protosolar cloud (Geiss & Gloeckler, 2003), to averages of approximately 100–200 × 10^{-6} for water ice accreted into carbonaceous chondrite parent bodies in the asteroid belt (e.g., Alexander et al., 2012; Piani et al., 2021), up to >500 × 10^{-6} for cometary ices in the outer Solar System (Müller et al., 2022). Studies of the H isotope composition of Solar System objects suggest that water D/H ratios are low in the warmer, inner parts of the Solar System, with deuterium enrichment globally increasing with heliocentric distance (e.g., Alexander et al., 2012; Drouart et al., 1999; Ito et al., 2022; Jacquet & Robert, 2013; Yang et al., 2013). Direct comparisons between different types of objects are, however, ambiguous; measured cometary D/H compositions may

© 2023 The Authors. *Meteoritics & Planetary Science* published by Wiley Periodicals LLC on behalf of The Meteoritical Society.
This is an open access article under the terms of the Creative Commons Attribution License, which permits use, distribution and reproduction in any medium, provided the original work is properly cited.

be affected by sublimation of water molecules between the nucleus and the tail of comets, whereas bulk chondrite D/H ratios correspond to complex mixtures of organics and hydrated minerals. In addition, the heliocentric distances at which the range of chondritic parent bodies accreted remain largely unconstrained.

Water in the cold (<30 K) molecular cloud from which the Solar System formed likely had a high D/H ratio, on the order of ~10^{-2}–10^{-3} (Ceccarelli et al., 2014). Following collapse of the cloud and protostar formation, the H isotope composition of water evolved throughout the protoplanetary disk, notably through isotopic exchange reactions such as $H_2O + HD \leftrightarrow HDO + H_2$ in warmer parts of the inner Solar System (e.g., Drouart et al., 1999; Jacquet & Robert, 2013; Yang et al., 2013). In addition, it is likely that D/H ratios of H present in H_2 gas and water ice varied temporally within a given region of the protoplanetary disk within the first few million years of Solar System evolution, due to changes in stellar output and disk structure (Ceccarelli et al., 2014; Hallis, 2017). Finally, early in the evolution of the protoplanetary disk following infall (<1 Myr), dust growth and inward drift from the outer Solar System could generate mixing between D-rich ices from the outer disk and D-depleted water in the inner disk (Jacquet & Robert, 2013; Yang et al., 2013). This allowed for the incorporation of D-rich water into asteroids forming within the snow line (the region beyond which it was cool enough for water ice to be stable).

This model of early mixing of ices in the Solar System is not, however, compatible with heterogeneities observed in heavier isotope systems such as O, Cr, and Ti across the Solar System, known as the isotope dichotomy (Kleine et al., 2020; Scott et al., 2018; Warren, 2011a, 2011b). This dichotomy suggests that, based on their isotopic compositions, the parent bodies of chondrites can be divided into two distinct groups: carbonaceous chondrites (CCs) from the outer Solar System and non-CCs (NCs; which include ordinary and enstatite chondrites) from the inner Solar System. It has been suggested that these planetesimals were originally divided into separate populations by Jupiter, and later scattered and congregated in the inner Solar System forming the present-day asteroid belt (Desch et al., 2018; Kruijer et al., 2017; Lichtenberg et al., 2021; Scott et al., 2018). Considering the overall expected trend of increasing D/H with heliocentric distance, one would expect a similar dichotomy in H isotope compositions, with CCs being more D-rich than NCs. However, NCs and CCs tend to span similar D/H ratios, and the highest meteorite D/H ratios are found in the least-altered unequilibrated ordinary chondrites (UOCs) (e.g., Alexander et al., 2012; Broadley et al., 2022; Deloule & Robert, 1995; Piani et al., 2015).

The vast majority of water and other volatile species in chondrites is found in the matrix, the fine-grained (<μm) interstitial material between larger objects such as chondrules, calcium-aluminum-rich inclusions (CAIs), Fe-Ni metal, and sulfides. There has been extensive work on water and its H isotope composition in CCs, due to their high matrix content (typically ~50 vol%, and up to >99 vol% for CI chondrites; e.g., Weisberg et al., 2006) and typically high H_2O abundances of up to ~13 wt% in CIs and CMs and ~8 wt% in Tagish Lake (Alexander et al., 2010; Piani et al., 2021; Rubin et al., 2007; Vacher et al., 2020). Despite ordinary chondrites (OCs) containing only ~10–15 vol% matrix (Weisberg et al., 2006), the least-metamorphosed samples can contain significant amounts of volatiles, such as water, as well as organic compounds, albeit in lower abundance than in volatile-rich CCs (e.g., Alexander et al., 1989; Dobrică et al., 2019; Piani et al., 2015; Sears et al., 1995; Vacher et al., 2020). Of particular interest for investigating water in the protoplanetary disk are the UOCs, which are classified as petrologic type 3.00–3.9, indicating that they have suffered little-to-no aqueous alteration and limited thermal metamorphism while on their parent bodies. This makes the least-metamorphosed type 3.00 UOCs some of the most pristine objects from the early Solar System. Unequilibrated ordinary chondrites show evidence for hydration in the matrix, characterized by the formation of secondary phyllosilicates, Ni-bearing sulfides, ferrous olivine, magnetite, as well as the presence of bleached chondrules (e.g., Alexander et al., 1989; Dobrică & Brearley, 2014; Grossman et al., 2000; Krot et al., 2006). A few studies have investigated the bulk mineralogy, water abundance, and H isotope composition of water in a number of important UOC samples of low petrologic subtypes such as Semarkona (LL3.00) and Bishunpur (LL3.15) (e.g., Alexander et al., 1989; McNaughton et al., 1982; Robert et al., 1987). However, a comprehensive inventory of the bulk water abundance and its H isotope composition in a range of type 3 UOC meteorites is yet to be established.

Previous investigations of the water inventory of UOCs yielded typical bulk H_2O abundances of up to ~1 wt%, accompanied by exceptionally high bulk D/H ratios ranging from 255 up to 700 × 10^{-6} in samples of the lowest petrologic types such as Semarkona and Bishunpur (e.g., Alexander et al., 1989, 2012; McNaughton et al., 1982; Robert et al., 1987; Yang & Epstein, 1983). Such bulk D/H ratios are much higher than those typical of terrestrial samples (bulk Earth D/H is approximately 149 × 10^{-6}; Lécuyer et al., 1998) and bulk D/H of water-rich CI, CM, and CR chondrites (~150–250 × 10^{-6}; Alexander et al., 2012; Piani et al., 2021; Vacher et al., 2020). In addition, in situ analyses of matrix areas in the LL3.00

19455100, 2023, 9, Downloaded from https://onlinelibrary.wiley.com/doi/10.1111/maps.14041 by NICE, National Institute for Health and Care Excellence, Wiley Online Library on [16/10/2026]. See the Terms and Conditions (https://onlinelibrary.wiley.com/terms-and-conditions) on Wiley Online Library for rules of use; OA articles are governed by the applicable Creative Commons License

Semarkona UOC showed that elevated H isotope signatures, with extreme D/H ratios up to approximately 1500–2000 × 10^{-6}, were carried by water-bearing minerals rather than C-rich organics (Deloule & Robert, 1995; Piani et al., 2015). Since asteroidal parent bodies from which UOCs originated formed closer to the Sun compared to the CI, CM, or CR chondrite parent bodies (Gaffey & Gilbert, 1998; Vernazza et al., 2015; Yoshikawa et al., 2007), the observation of higher bulk D/H ratios in the most pristine UOCs compared to carbonaceous chondrites appears at odds with current models where water D/H ratios increase with heliocentric distance. This suggests that either there is something unusual about the few UOC samples that have elevated bulk D/H ratios, or that current models of water processing and D/H evolution in the protosolar nebula are incomplete.

To further assess whether UOCs of the lowest petrologic subtypes are indeed characterized by elevated D/H ratios, and to determine how water abundance and D/H ratios evolve with incipient metamorphism, we measured bulk water abundances and associated H isotope compositions in a comprehensive set of 21 type 3 OC samples. To complement these data, we also determined the bulk mineralogical composition of 19 of these samples in order to assess the possible phase(s) hosting water.

MATERIALS AND METHODS

Samples

The samples analyzed in this study were Aba Panu, Bishunpur, Bo Xian, Bremervörde, Ceniceros, Chainpur, Dhajala, El Médano 260, Krymka, Mezö-Madaras, Ngawi, Northwest Africa (NWA) 11534, NWA 11752, NWA 4560, Paposo 004, Parnallee, San Juan 055, Semarkona, Sharps, St Mary's County, and Tieschitz. This sample set comprises of 15 falls and six finds, ranging from H to LL groups and petrologic types 3.00–3.9 (details in Table 1). For each meteorite, ~11–85 mg chips were finely ground to produce powdered samples with grain sizes on the order of microns, which were then stored in a desiccator to undergo degassing and isotope analysis <2–3 days after crushing.

Bulk Chondrite Water Abundance and H Isotope Composition

Bulk chondrite water abundances and H isotope compositions were determined on 5–10 mg aliquots of each meteorite using the Thermo Scientific Elemental Analyzer (EA) IsoLink—deltaV Isotope Ratio Mass Spectrometer (IRMS) system at the Centre de Recherches Pétrographiques et Géochimiques (CRPG) laboratory in Nancy, France. To minimize the effect of adsorption of terrestrial water onto the powdered samples on their H_2O abundances and H isotope compositions, samples were weighed in tin capsules that were loaded into a sample carousel and degassed under vacuum at 120°C for 48 h in a degassing canister. After dehydration, the degassing canister was opened in a dry N_2-flushed glove box, the sample carousel was transferred into a sealed autosampler pre-flushed with He, connected to the EA, and pumped out for 20 min before opening it to the reduction column. This technique prevents any contact with atmospheric H, and thus potential rehydration, after the pre-degassing step. The samples were combusted at 1450°C in a glassy carbon reaction tube filled with glassy carbon chips. The gases produced were separated on a chromatographic column maintained at 60°C and the H_2 obtained was entered into the mass spectrometer through an open split for D/H isotopic composition analysis (see Vacher et al. (2020) and Piani et al. (2020) for further details). The following standards were routinely measured throughout: Mica-Mg (δD = −76.5‰, H_2O = 2.58 wt%), SO188—fine-grained marine sediment (δD = −84.6‰, H_2O = 4.36 wt%), MuscD65—muscovite (δD = −90.0‰, H_2O = 4.44 wt%), and GSJ_JB1/GSL_JB3—two basalts (δD = −102.9‰, H_2O = 1.02 wt % and δD = −97.9‰, H_2O = 0.20 wt%, respectively). Uncertainties on H_2O abundances and D/H ratios were taken as 12% and 5‰ (2σ) based on repeated measurements of standards with similar water concentration as the samples. Estimates of the reproducibility for the range of concentrations measured are 10%–15% at 2σ. The H isotope compositions are reported using the δD notation, which corresponds to the deviation of the measured D/H ratios from the standard mean ocean water (SMOW) in parts per thousand (‰; $\delta D = ([D/H_{measured}/D/H_{SMOW}] - 1) \times 1000$, with $D/H_{SMOW} = 155.76 \times 10^{-6}$).

Bulk Chondrite Mineralogy

The mineralogy of 19 of the UOC samples (there was insufficient material for Semarkona and Bo Xian) was characterized using X-ray diffraction (XRD) at the Natural History Museum (NHM), London. For initial phase identification, a few milligrams of each powder was mixed with a small amount of acetone and smeared onto a low-background single-crystal sapphire substrate. XRD patterns were then collected with Cu K_1 radiation for up to ~17 h using an INEL X-ray diffractometer and a curved 120° position-sensitive detector (PSD) in a fixed geometry relative to the primary X-ray beam. Silicon and silver behenate were used for calibration, and phases in the meteorites were identified using the International Centre for Diffraction Data (ICDD) database (PDF-2).

19455100, 2023, 9, Downloaded from https://onlinelibrary.wiley.com/doi/10.1111/maps.14041 by NICE, National Institute for Health and Care Excellence, Wiley Online Library on [16/10/2026]. See the Terms and Conditions (https://onlinelibrary.wiley.com/terms-and-conditions) on Wiley Online Library for rules of use; OA articles are governed by the applicable Creative Commons License

TABLE 1. Bulk H_2O abundance and D/H ratios for unequilibrated ordinary chondrites.

Meteorite	Type	Source[a]	#	Fall	Weathering grade (finds)	Mass (mg)	H_2O (wt%)	±	D/H ($\times 10^{-6}$)	δD (‰)	±
Ngawi	LL3.1–3.7[b]	USNM	USNM 2483	Yes		7.75	0.61	0.07	333.91	1144	5
Semarkona	LL3.00	AMNH	AMNH 4128	Yes		9.46	0.90	0.11	383.09	1460	5
NWA 11752	LL3.05	CEREGE	K 340	No	W3	5.09	1.36	0.16	202.99	303	5
Bishunpur	LL3.15	NHM	BM.80339	Yes		6.35	0.91	0.11	273.47	756	5
NWA 11534	LL3.15	CEREGE	K 324	No	W2	5.65	1.10	0.13	150.27	−35	5
Krymka	LL3.2	NHM	BM.1956,325	Yes		5.72	0.80	0.10	166.07	66	5
NWA 4560	LL3.2	CEREGE	n/a	No	W2	8.25	1.43	0.17	150.06	−37	5
St Mary's County	LL3.3	USNM	USNM 5930	Yes		5.95	0.99	0.12	145.33	−67	5
Chainpur	LL3.4	NHM	BM.1915,86	Yes		6.89	0.45	0.05	180.65	160	5
Parnallee	LL3.6	NHM	BM.1985, M138	Yes		6.89	0.42	0.05	139.26	−106	5
Bo Xian	LL3.9	NHM	BM.1999,M19	Yes		10.19	0.08	0.01	142.9	−83	5
El Médano 260	L3.10	CEREGE	M 382	No	W4	7.32	1.43	0.17	175.73	128	5
Paposo 004	L3.1	CEREGE	n/a	No		8.54	0.57	0.07	145.18	−68	5
Aba Panu	L3.6		n/a	Yes		9.95	0.09	0.01	141.18	−94	5
Ceniceros	L3.7	NHM	BM.1989,M31	Yes		8.68	0.70	0.08	136.51	−124	5
Mezö-Madaras	L3.7	NHM	BM.33909	Yes		7.82	0.27	0.03	140.52	−98	5
Tieschitz	H/L3.6	NHM	BM.2003,M12	Yes		9.70	0.25	0.03	221.52	422	5
Bremervörde	H/L3.9	NHM	BM.33910	Yes		10.20	0.37	0.04	146.2	−61	5
San Juan 055	H3.2–3.5	CEREGE	SJ 055	No	W2	7.82	1.35	0.16	133.94	−140	5
Sharps	H3.4	USNM	USNM 640	Yes		7.86	0.58	0.07	165.96	65	5
Dhajala	H3.8	NHM	BM.1976,M12	Yes		10.33	0.06	0.01	138.16	−113	5

Uncertainties are given at the 2σ level.

[a]Museum sources are as follows: AMNH, American Museum of Natural History, New York (USA); CEREGE, Centre Européen de Recherche et d'Enseignement des Géosciences de l'Environnement, Aix-en-Provence (France); NHM, Natural History Museum, London (UK); USNM, Smithsonian National Museum of Natural History, Washington (USA).

[b]Ngawi is a breccia with lithologies of 3.1 and 3.6/3.7 (Grossman & Brearley, 2005; Sears et al., 1991).

These measurements will be referred to as the "low flux" XRD analyses, or LF-XRD.

The modal mineralogy of seven of the lowest petrologic type UOC falls (Bishunpur, Ngawi, Krymka, St Mary's County, Chainpur, Parnallee, and Tieschitz) was determined using a PSD-XRD equipped with a MicroSource high-brightness X-ray generator, which can deliver a focused beam of X-rays with a high flux (see Bland et al. (2004) for details). These measurements will be referred to as the micro-XRD. For these analyses, ~1–2 mg of the remaining powder (i.e., not mixed with acetone) was loaded into a zero-background microwell using a stainless steel spatula. The powder was then pressed fully into the microwell using a glass slide, with any excess material removed from around the edges of the well. Pressing the powder into the microwell can impart preferred crystal orientations, which were identified by manual inspection of the data. Diffraction patterns were collected using Cu radiation, with the primary X-ray beam focused onto the sample using a 100 μm pinhole. Each sample was analyzed for 2 h, during which it was continuously rotated. Standards of minerals identified in the meteorites were prepared in the same way and analyzed for 10 min.

Mineral abundances were determined using a pattern-stripping procedure previously described in detail by Batchelder and Cressey (1998), Schofield et al. (2002), Bland et al. (2004), and Howard et al. (2009). Briefly, XRD patterns of the mineral standards were scaled to the same measurement time as the meteorites (i.e., ×12) and reduced by a factor to fit peak intensities in an individual meteorite pattern. When the sum of the fit factors reached one, the mineral standard patterns were subtracted from the meteorite pattern to leave a residual with no peaks and approximately zero counts. The fit factors were then corrected for relative differences in X-ray absorption to give the final abundance of each phase in the meteorite. Detection limits are on the order of 1 wt% (depending on the specific phase) and the estimated uncertainties on the calculated abundances are up to ~5 wt% (e.g., King et al., 2015).

19455100, 2023, 9, Downloaded from https://onlinelibrary.wiley.com/doi/10.1111/maps.14041 by NICE, National Institute for Health and Care Excellence, Wiley Online Library on [16/10/2026]. See the Terms and Conditions (https://onlinelibrary.wiley.com/terms-and-conditions) on Wiley Online Library for rules of use; OA articles are governed by the applicable Creative Commons License

RESULTS

Bulk Water Abundance and H Isotope Composition

The bulk H_2O abundances of the 21 studied UOCs vary from 0.06 to 1.43 wt%, with samples of the lowest petrologic subtypes typically having the highest water abundances (Table 1, Figure 1). As shown in Figure 1, many of the finds have H_2O abundances around 1.4 wt%, notably higher than their fall counterparts that contain up to 1 wt% H_2O. Figure 2 shows that the majority of UOCs analyzed have δD values between −200‰ and +200‰. For comparison, the typical D/H composition of terrestrial water in deserts where the finds were recovered is between about 0‰ and −40‰ (as represented by the gray band in Figure 2; Hallis et al., 2015; Lécuyer et al., 1998). Five meteorites have bulk δD values significantly higher than +200‰: One find has a bulk δD value of +303‰ (NWA 11752, LL3.05) and four falls have bulk δD values of 422‰ (Tieschitz, H/L 3.6), 756‰ (Bishunpur, LL3.15), 1144‰ (Ngawi, LL3.1–3.7), and 1460‰ (Semarkona, LL3.00). There is a general trend of decreasing D/H ratios with increasing petrologic subtype, with the exception of Tieschitz, which is classified as petrologic subtype 3.6. Ngawi, which has one of the highest bulk D/H ratios, is a breccia containing two distinct lithologies of LL3.1 and LL3.6/3.7 (Grossman & Brearley, 2005; Sears et al., 1991). Excluding the finds, the sample set displays a rough trend of increasing bulk D/H ratios with increasing H_2O abundance. Although not illustrated in Figure 2, there is no apparent relationship between the H_2O abundance and/or D/H ratios and the different UOC groups (Table 1).

Bulk Chondrite Mineralogy

The bulk chondrite LF-XRD patterns for all UOCs are similar and indicate that the major constituents of these meteorites are olivine (with variable Mg/Fe contents) and pyroxene (mainly low-Ca), with lesser amounts of Fe-sulfide (troilite) and metal (Figure 3). Minor plagioclase is also likely present in some meteorites (e.g., Lewis et al., 2022), but identification was challenging because its main diffraction peaks overlap with those from the more abundant olivine and pyroxene. No diffraction peaks from phyllosilicates are observed above the background in any of the UOCs; however, there is a magnetite peak in the XRD pattern for Ngawi (Figure 3), and all of the finds have a peak attributed to goethite.

The quantitative modal mineralogy of Bishunpur, Ngawi, Krymka, St Mary's County, Chainpur, Parnallee, and Tieschitz determined with micro-XRD confirms the relatively high abundances of olivine and pyroxene (Table 2 and Table S1). In these meteorites, olivine abundances range from 41 to 71 wt% (average = 57.8 wt %) and pyroxene abundances from 23 to 49 wt% (average = 34.2 wt%), in good agreement with previous studies of ordinary chondrite mineralogy using PSD-XRD (Dunn et al., 2010; Menzies et al., 2005). Olivine compositions appear to become more homogenized with increasing petrologic type (see Table S1), although we note that our data set includes a limited number of samples. Abundances for Fe-sulfide and metal (<5 wt%) are generally a little lower than those reported for ordinary chondrites by Menzies et al. (2005) and Dunn et al. (2010), who mainly analyzed higher petrologic types. We also determined that Ngawi contains 4 wt% magnetite.

Bishunpur and Krymka differ from the other samples in that, during the quantitative phase analysis, we found that following subtraction of the crystalline phases (e.g., olivine, pyroxene, etc.) from the XRD pattern, the sum of the fit factors was less than one. This is consistent with the presence of a poorly crystalline ("amorphous"), Fe-bearing component, which will fluoresce due to the use of Cu radiation and, therefore, contribute to the background of the XRD pattern (e.g., Bland et al., 2004; King et al., 2015). Candidate phases in ordinary chondrites include Fe-rich weathering products (e.g., "rusts"), phyllosilicates/clays (e.g., Menzies et al., 2005), amorphous silicates (e.g., Dobrică & Brearley, 2020), and/or chondrule glass (e.g., Krot & Rubin, 1994; Lewis et al., 2022; Lewis & Jones, 2019). For Bishunpur and Krymka, we attempted to fit the intensity and overall shape of the remaining residuals using a combination of our Fe-(oxy)hydroxide, serpentine–smectite, and synthetic amorphous silicate standards and, in both cases, found reasonable agreement with the phyllosilicates (when scaled and excluding the diffraction peaks). We cannot fully rule out a contribution from rusts and amorphous silicates/glass but note that Menzies et al. (2005) also detected phyllosilicates in Bishunpur using micro-XRD. We determined X-ray "amorphous" abundances of ~16 wt% in Bishunpur and ~12 wt% in Krymka by using the X-ray absorption coefficient calculated by Menzies et al. (2005) for ordinary chondrite phyllosilicate compositions.

DISCUSSION

To obtain a more comprehensive picture of early water transport in the protoplanetary disk, we have investigated the OCs, which are less well studied than CCs. First, we discuss the bulk mineralogy of OCs, including identification of potentially hydrated minerals, obtained through XRD. This helps to understand the bulk H_2O contents and H isotope compositions we measured on these same OC samples.

19455100, 2023, 9, Downloaded from https://onlinelibrary.wiley.com/doi/10.1111/maps.14041 by NICE, National Institute for Health and Care Excellence, Wiley Online Library on [16/10/2026]. See the Terms and Conditions (https://onlinelibrary.wiley.com/terms-and-conditions) on Wiley Online Library for rules of use; OA articles are governed by the applicable Creative Commons License

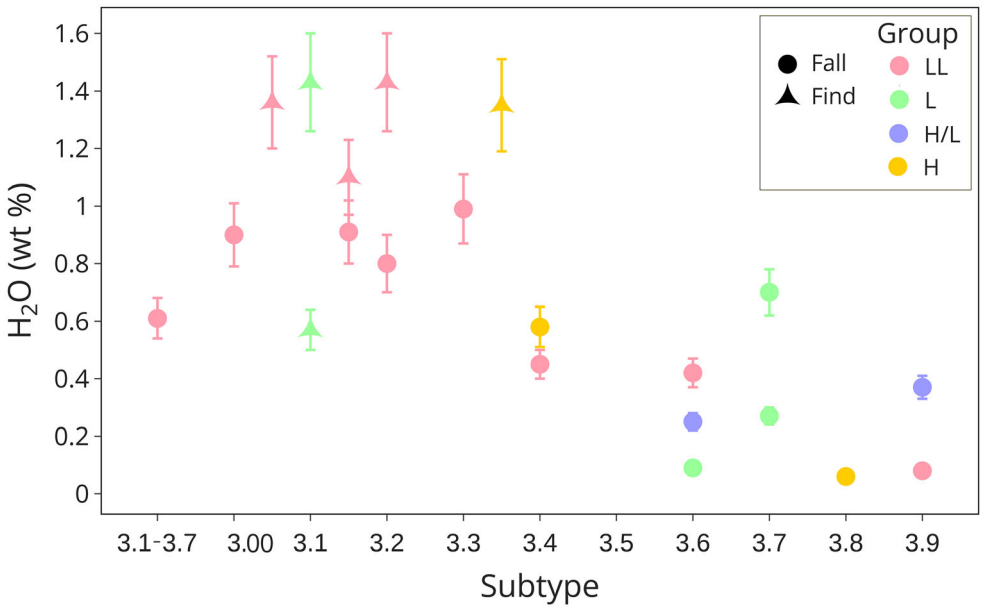

FIGURE 1. Bulk H_2O content of UOCs as a function of petrologic subtype. The sample with petrologic type 3.1–3.7 is Ngawi, a brecciated LL chondrite. (Color figure can be viewed at wileyonlinelibrary.com)

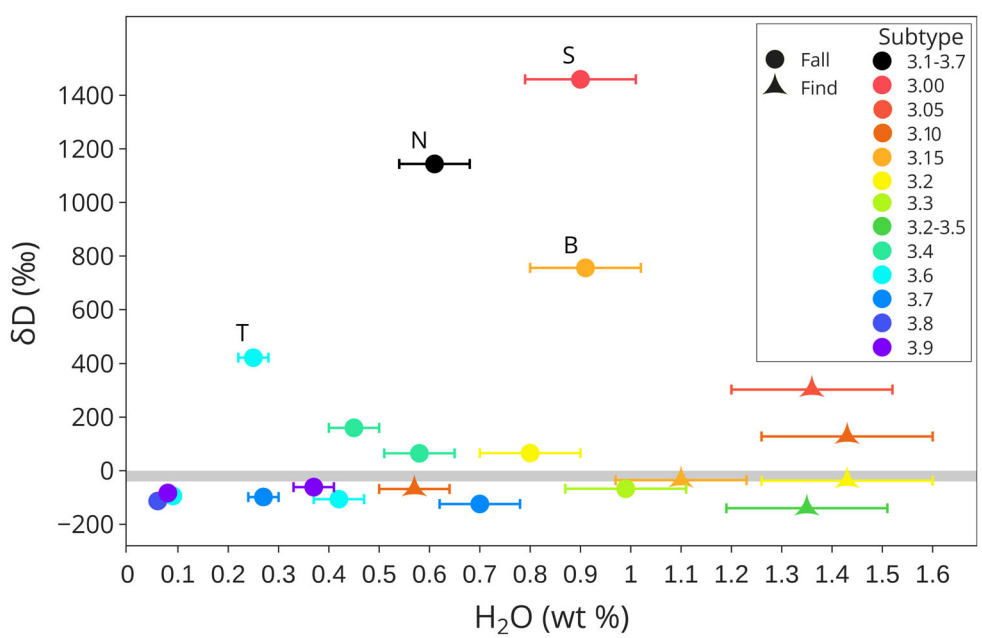

FIGURE 2. Bulk H isotope composition as a function of water abundance. The gray band spanning from −40‰ to 0‰ represents the mean D/H ratio of Earth desert water, where all the finds were collected (Lécuyer et al., 1998). S, Semarkona; N, Ngawi; B, Bishunpur; T, Tieschitz. Colors represent petrologic subtypes, where Ngawi is labeled as 3.1–3.7 and San Juan 055 as 3.2–3.5 as they are breccias with multiple lithologies. Uncertainties on δD values are smaller than the size of the symbols (±5‰). (Color figure can be viewed at wileyonlinelibrary.com)

Bulk Mineralogy of Type 3 Ordinary Chondrites

Overall, the XRD patterns of 19 bulk UOCs and the calculated modal mineralogy of seven of these meteorites (Table 2, Figure S1) are all similar and generally consistent with known OC mineralogy and abundances (e.g., Brearley & Jones, 1998; Huss et al., 2006). In particular, the XRD patterns and mineral abundances are

19455100, 2023, 9, Downloaded from https://onlinelibrary.wiley.com/doi/10.1111/maps.14041 by NICE, National Institute for Health and Care Excellence, Wiley Online Library on [16/10/2026]. See the Terms and Conditions (https://onlinelibrary.wiley.com/terms-and-conditions) on Wiley Online Library for rules of use; OA articles are governed by the applicable Creative Commons License

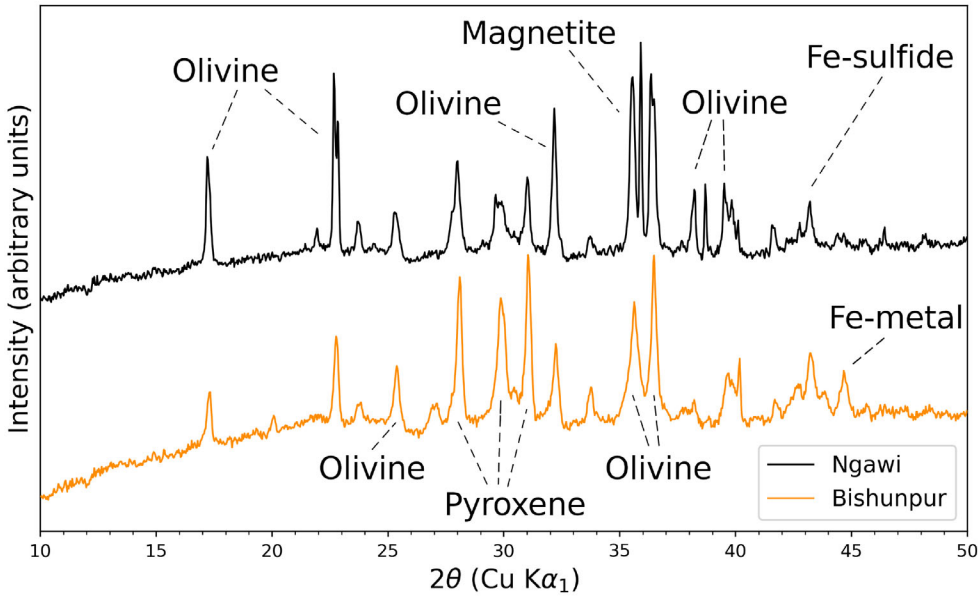

FIGURE 3. Micro-XRD patterns of Bishunpur and Ngawi. Patterns for all the UOCs analyzed in this study are similar, with the main diffraction peaks originating from olivine, pyroxene, Fe-sulfide, and metal. A peak attributed to magnetite was observed for Ngawi. (Color figure can be viewed at wileyonlinelibrary.com)

TABLE 2. Modal mineralogy (in wt%) determined by high flux XRD for seven UOC falls.

Name	Subtype	Olivine[a]	Pyroxene[b]	Fe-sulfide[c]	Metal[d]	Magnetite	X-ray "amorphous"[e]
Ngawi	LL3.1–3.7	71	23	2	n.d.	4	n.d.
Bishunpur	LL3.15	41	39	3	1	n.d.	16
Krymka	LL3.2	54	32	2	1	n.d.	12
St Mary's County	LL3.3	48	49	3	<1	n.d.	n.d.
Chainpur	LL3.4	71	25	3	1	n.d.	n.d.
Parnallee	LL3.6	67	29	3	1	n.d.	n.d.
Tieschitz	H/L3.6	53	43	3	1	n.d.	n.d.

Uncertainties are up to ~5 wt% (e.g., King et al., 2015).
[a]Sum of Fo_{40}–Fo_{100} in 20% increments.
[b]Sum of enstatite and augite.
[c]Troilite.
[d]Kamacite, $Fe_{90}Ni_{10}$.
[e]Determined using the phyllosilicate X-ray absorption coefficient from Menzies et al. (2005), but could also include pristine amorphous silicates, rusts, and/or chondrule glass.

in good agreement with those determined for UOCs (10's mg of sample) by Menzies et al. (2005). Considering the two data sets together (12 UOCs in total from petrologic types 3.1–3.8), there is a weak trend of olivine compositions spanning a wider range in lower petrologic type meteorites (~Fo_{20} – Fo_{100}) and becoming homogenized with thermal metamorphism (~Fo_{60} to Fo_{80} in types >3.6). Minor phases such as Fe-sulfide and metal do not show any systematic changes in abundance with petrologic type. Menzies et al. (2005) also observed 5.9–15.1 wt% plagioclase in UOCs of petrologic types ≥3.3, but we were unable to identify any plagioclase peaks definitively in the samples we studied.

We identified a small amount of magnetite (4 wt%) in Ngawi, which is consistent with the petrographic observations of Choi et al. (1998) and Krot et al. (2022) and suggests aqueous alteration of metallic and sulfide phases on the asteroid parent body. Magnetite has also been identified by electron microscopy in other UOCs including Krymka (Semenenko et al., 2001) and Tieschitz (Huss et al., 1981; Wood, 1962), while Menzies et al. (2005) estimated magnetite abundances of ≤1 wt% in Semarkona, Chainpur, Parnallee, and Mezö-Madaras by Mössbauer spectroscopy. We did not find compelling evidence for magnetite in the XRD patterns for any of these meteorites; however, at such low abundances, the

19455100, 2023, 9, Downloaded from https://onlinelibrary.wiley.com/doi/10.1111/maps.14041 by NICE, National Institute for Health and Care Excellence, Wiley Online Library on [16/10/2026]. See the Terms and Conditions (https://onlinelibrary.wiley.com/terms-and-conditions) on Wiley Online Library for rules of use; OA articles are governed by the applicable Creative Commons License

detection of magnetite is hampered by the overlap of its main diffraction peak with those from the abundant olivine in the samples.

Possible further evidence for hydration of the OC parent body comes from the detection of X-ray "amorphous" components in Bishunpur and Krymka that could be related to phyllosilicates. The presence of poorly crystalline phyllosilicates in Bishunpur is supported by in situ observations of the matrix (Alexander et al., 1989; Hutchison et al., 1987), with Menzies et al. (2005) reporting a phyllosilicate abundance of ~20 wt%, comparable to the X-ray "amorphous" component (~16 wt%) in our Bishunpur sample. However, it is worth noting that unlike the study by Menzies et al. (2005), there were no observable smectite peaks in this analysis and this value is determined from the residual XRD pattern following deconvolution. These elevated phyllosilicate abundances may also indicate the presence of pervasive incipient alteration channels in ferromagnesian silicates (Menzies et al., 2005). In addition, Bishunpur has one of the highest bulk H_2O contents (~1 wt%) of the UOC falls we analyzed (Table 1 and Figure 2). Similarly, although we were unable to acquire XRD patterns of Semarkona, it contains ~0.9 wt% H_2O and previous studies have identified phyllosilicates in the matrix (Hutchison et al., 1987) and estimated a bulk phyllosilicate abundance of ~15 wt% (Menzies et al., 2005).

The petrographic evidence for the presence of phyllosilicates in Krymka is less conclusive; although phyllosilicates have been previously reported in this sample, it is to a significantly lesser extent than that of Bishunpur (Semenenko et al., 2005; Weisberg et al., 1997). Nevertheless, we find that Krymka has a bulk H_2O content of ~0.8 wt%, which is comparable to Semarkona and suggests that a hydrous phase is present in the meteorite. Terrestrial weathering products are unlikely as Krymka is a fall and we found that our Fe-(oxy) hydroxide standards were not a good match for the background intensity of the XRD pattern. Amorphous silicates and/or chondrule glass are possible but are not expected to host significant quantities of H_2O, whereas phyllosilicates can contain ~15–20 wt% H_2O.

Bulk Chondrite Water Contents

Ordinary chondrites exhibit signs of both thermal alteration, spanning from petrologic types 3.00 to 7 (e.g., Huss et al., 2006), and aqueous alteration, typically identified in type 3 UOCs by the presence of secondary phases formed through hydrothermal alteration, such as phyllosilicates (Alexander et al., 1989), amphiboles (Dobrică & Brearley, 2014), fayalite and magnetite (Dobrică et al., 2019; Krot et al., 1997), and bleached chondrules (Grossman et al., 2000). Figures 1 and 4 show that UOC falls with petrologic types <3.4 contain up to approximately 1 wt% H_2O, and that bulk H_2O abundances then decrease with increasing metamorphic grade. Increasing subtype reflects increasing thermal metamorphism, resulting in the breakdown of phyllosilicates at temperatures $\gtrsim$700 K (Velbel & Zolensky, 2021; Wolters & Emmerich, 2007). UOCs of the lowest subtypes (≤3.2) are not thought to have undergone peak temperatures higher than 500 K, allowing for the survival of phyllosilicates in these samples (Alexander et al., 1989; Lewis & Jones, 2019). UOCs of higher subtypes are thought to have undergone prolonged periods of heating at peak temperatures of ~900 K (Lewis et al., 2022), causing dehydroxylation of any phyllosilicates originally present. This observation is also in agreement with the negligible abundance of XRD amorphous components in UOC samples with subtypes >3.2–3.3.

There is no clear link between bulk UOC water abundances and OC chondritic H, L, and LL groups (Figure 1). Among the samples analyzed here, bulk water abundances and/or H isotope compositions have been analyzed previously in Semarkona (LL3.00), Bishunpur (LL3.15), Chainpur (LL3.4), Parnallee (LL3.6), and Ngawi (LL3.6) (Alexander et al., 2012; McNaughton et al., 1982; Robert et al., 1979, 1987). Figure 4 shows that bulk water abundances measured for a given sample vary, and that bulk water abundances measured here tend to be higher than most literature data, notably for Semarkona, Bishunpur, and Chainpur. The bulk H_2O abundance obtained for Semarkona is similar to that of Alexander et al. (2012) (Figure 4). The cause for such variability for a given sample is unclear; one possibility is a sampling effect, where bulk samples including variable amounts of matrix would result in variable bulk H_2O abundances. As there appear to be somewhat systematic differences between the data sets, it is also possible that differences in sample preparation, storage, and analytical techniques used may all be factors. For example, the maximum combustion temperature in this study is higher than that of the studies by McNaughton et al. (1981, 1982) and Yang and Epstein (1983), and our study utilized a single combustion as opposed to stepwise pyrolysis.

As previously mentioned, ordinary chondrites have lower abundances of fine-grained matrix compared to carbonaceous chondrites, with UOCs comprising on average ~10–15% matrix (Grossman & Brearley, 2005), as opposed to ~50% in most CCs, and up to almost 100% for some hydrated CCs (Weisberg et al., 2006). Making the simplified assumption that all the water in UOCs is in the matrix, utilizing matrix abundances from Grossman and Brearley (2005), or where unavailable assuming that samples have a matrix abundance of 10%,

19455100, 2023, 9, Downloaded from https://onlinelibrary.wiley.com/doi/10.1111/maps.14041 by NICE, National Institute for Health and Care Excellence, Wiley Online Library on [16/10/2026]. See the Terms and Conditions (https://onlinelibrary.wiley.com/terms-and-conditions) on Wiley Online Library for rules of use; OA articles are governed by the applicable Creative Commons License

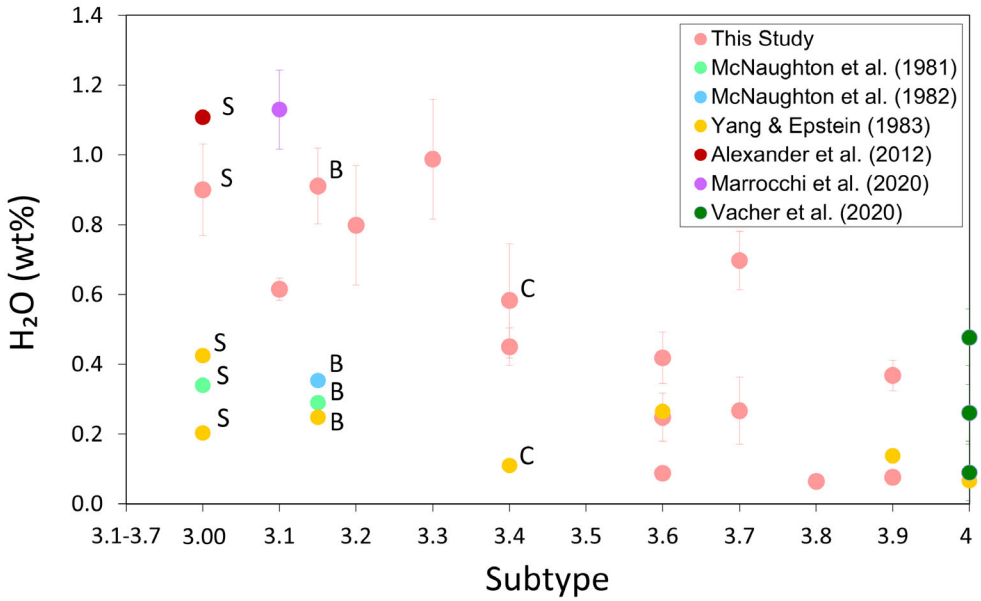

FIGURE 4. Bulk H_2O content versus subtype, including literature data (Alexander et al., 2012; Marrocchi et al., 2020; McNaughton et al., 1981, 1982; Vacher et al., 2020; Yang & Epstein, 1983). Samples with duplicate measurements are labeled S (Semarkona), B (Bishunpur), and C (Chainpur). (Color figure can be viewed at wileyonlinelibrary.com)

and using H_2O abundances from Table 1, we estimate the water abundance of the matrix at 4.8–8.2 wt% H_2O for UOC falls ≤3.3 (Figure 5). This is comparable to the calculated matrix water contents, as determined using bulk water contents and individual chondrite matrix abundances, of some phyllosilicate-rich CR and CM chondrites (Figure 5), where the CM chondrites with the lowest H_2O values and least parent body alteration are Paris (CM2.7; Piani & Marrocchi, 2018) and Asuka 12,236 (CM2.9; Marrocchi et al., 2023). Of note, we measured the highest water abundance in St Mary's County, which has a terrestrial-like D/H ratio. We suggest this sample may have become terrestrially altered, similar to the finds. UOC falls with subtypes >3.3 are much closer in estimated matrix water contents to the phyllosilicate-poor CV chondrites, whose matrix is mostly anhydrous (e.g., Alexander et al., 2010; Piani & Marrocchi, 2018; Vacher et al., 2020). This suggests that the OC parent bodies likely underwent significant aqueous alteration, albeit to a lesser degree than what is observed in many CM and CR chondrites, prior to thermal metamorphism.

UOC finds have higher H_2O abundances relative to fall counterparts of the same subtype (Figure 1). This suggests that finds, which have resided at the Earth's surface for unknown periods of time, have absorbed terrestrial water prior to being collected. H_2O abundances in finds increase with weathering grade and all finds had a feature in their XRD patterns associated with goethite. Excluding the single find with an H_2O content of ~0.6 wt%, which has the lowest weathering grade, most of the finds have a similar bulk H_2O abundance of ~1.4 wt%. This may be indicative of a general limit to the amount of terrestrial water that UOCs can uptake.

Bulk Hydrogen Isotope Composition of UOCs

Meteorite finds tend to have lower δD values than meteorite falls of the same petrologic type (Figure 2). This suggests that any extraterrestrial water originally hosted in hot desert meteorite finds has equilibrated with terrestrial water. In future studies of water in unequilibrated ordinary chondrites, and meteorites in general, it is thus recommended to prioritize falls over finds.

Two of the highest bulk D/H ratios are measured in the lowest subtype UOCs (<3.2), with δD values of 756‰ and 1460‰ for Bishunpur and Semarkona, respectively (Table 1, Figures 2 and 6). This tends to be at the lower end of previous bulk D/H ratios measured in these two samples (e.g., Alexander et al., 2012; McNaughton et al., 1981, 1982; Yang & Epstein, 1983; Figure 6). The lower H_2O abundances measured in the 1980s' studies compared to our bulk analyses (Figure 4) may indicate that the earlier studies did not sample the complete UOC D/H inventory. Bulk δD values decrease swiftly between petrological subtypes 3.00 and 3.4 (except for Tieschitz, which we discuss below), suggesting that the phase(s) hosting elevated D/H ratios is easily destroyed or altered with minor thermal

19455100, 2023, 9, Downloaded from https://onlinelibrary.wiley.com/doi/10.1111/maps.14041 by NICE, National Institute for Health and Care Excellence, Wiley Online Library on [16/10/2026]. See the Terms and Conditions (https://onlinelibrary.wiley.com/terms-and-conditions) on Wiley Online Library for rules of use; OA articles are governed by the applicable Creative Commons License

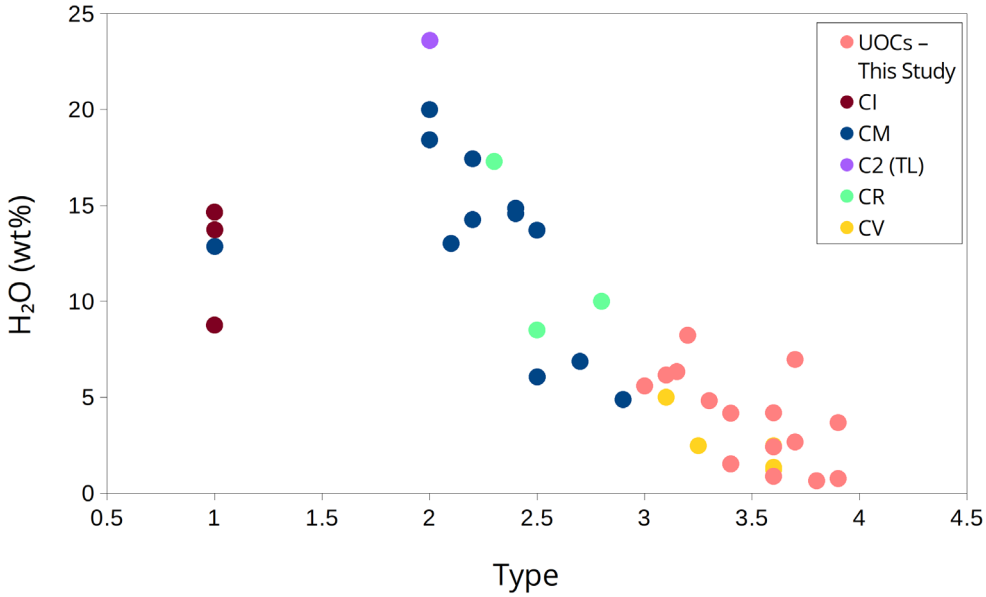

FIGURE 5. Calculated matrix H_2O abundance versus petrologic type (combining bulk H_2O abundances and matrix abundances of 10% for OCs and 40%–99% for CCs, based off groups or, where available, individual samples). Data from this study (falls only) are represented in pink and all other points are CC literature data (Alexander et al., 2010, 2013; Marrocchi et al., 2023; Piani & Marrocchi, 2018; Vacher et al., 2020; Weisberg et al., 2006), with CM and CV subtype classifications by Rubin et al. (2007) and Bonal et al. (2004), respectively. TL, Tagish Lake. In this plot, Ngawi (3.1–3.7) is classified as 3.1. (Color figure can be viewed at wileyonlinelibrary.com)

alteration (e.g., Vacher et al., 2020). The breccia Ngawi has the second highest bulk D/H ratio, with a δD value of 1140‰ (Figure 6), confirming that our sample is dominated by a low subtype lithology.

Previous in situ H isotope studies in UOCs (e.g., Semarkona, Bishunpur, and Krymka) have revealed the presence of deuterium-rich "hotspots" within the hydrated matrices and/or insoluble organic matter (IOM) component present in the samples (Alexander et al., 2010; Deloule & Robert, 1995; Piani et al., 2015; Remusat et al., 2016), with large δD variations of several thousands of permil observed at the micrometer scale within the matrix of Semarkona (Deloule & Robert, 1995; Piani et al., 2015). Several processes have been suggested to explain this type of extreme small-scale heterogeneity, which is also observed in CCs, including H isotope fractionation as a result of photodissociation within a plasma, as has previously been shown to produce D/H heterogeneity in CC IOM (Robert et al., 2017), or inheritance from the molecular cloud or protoplanetary disk (Busemann et al., 2006). As we analyzed homogenized bulk powders, the matrix H component is diluted, masking these extreme variations observed at the microscale. For example, Krymka has a low bulk δD value of 66‰, despite being a subtype 3.2 and hosting IOM with δD values of up to ~2500‰ similar to that of Semarkona (Alexander et al., 2010; Piani et al., 2015).

Deciphering the mechanism(s) that caused bulk D/H ratios to decrease with increasing thermal metamorphism is not straightforward. Globally, this bulk D/H decrease is accompanied by a progressive loss of water, indicating an open system process. For example, it has been suggested that degassing of H_2 produced by iron oxidation in a hydrated parent body preferentially leaves behind D-rich material that would generate bulk D enrichments with increased heating and oxidation intensity, possibly explaining D-rich hotspots observed in IOM in Semarkona, Bishunpur, Krymka, Chainpur, and Tieschitz (e.g., Alexander et al., 2007, 2010). However, D enrichment with increasing metamorphism is contrary to what we measure in bulk UOCs. Importantly, bulk rock D/H analyses comprise contributions from hydrated silicates, as well as from H-bearing organics and any other H-bearing phase present. In UOCs, IOM is characterized by elevated δD values of >2000‰ (Alexander et al., 2007). Elevated D/H ratios in low subtype UOCs may, thus, indicate a dominant contribution from IOM, progressively diminishing with thermal metamorphism. However, this is not consistent with in situ studies of Semarkona matrix, which indicate that the highest D/H ratios are not hosted by IOM (Deloule & Robert, 1995; Piani et al., 2015). In addition, Semarkona and Bishunpur contain 0.36 and 0.25 wt% bulk C, corresponding to 0.64 and 0.43 wt% IOM, respectively, assuming all C is hosted in IOM with C abundances of

19455100, 2023, 9, Downloaded from https://onlinelibrary.wiley.com/doi/10.1111/maps.14041 by NICE, National Institute for Health and Care Excellence, Wiley Online Library on [16/10/2026]. See the Terms and Conditions (https://onlinelibrary.wiley.com/terms-and-conditions) on Wiley Online Library for rules of use; OA articles are governed by the applicable Creative Commons License

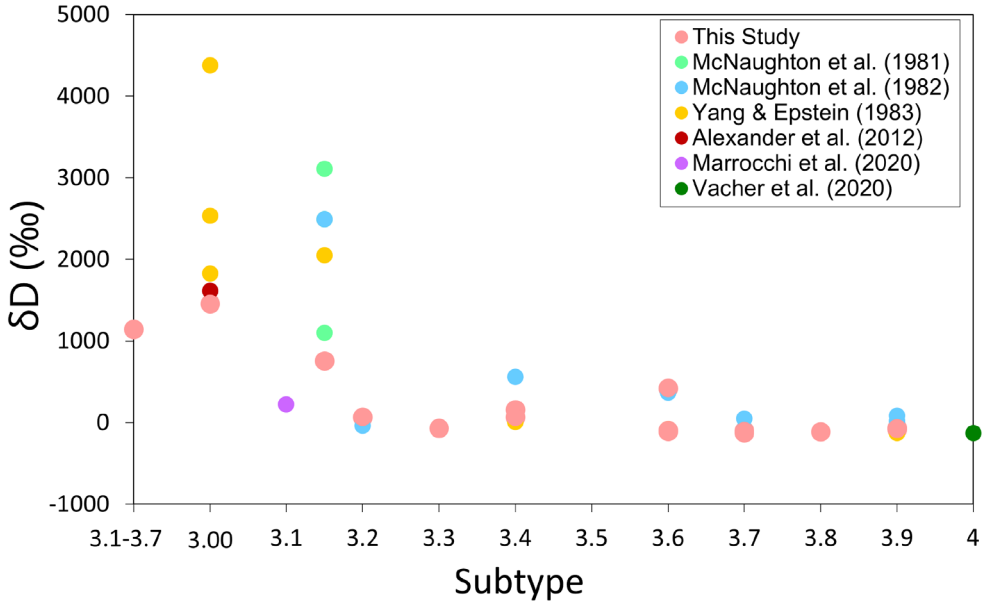

FIGURE 6. Bulk δD versus subtype, comparing data from this study with previous bulk UOC analyses (Alexander et al., 2012; Marrocchi et al., 2020; McNaughton et al., 1981, 1982; Vacher et al., 2020; Yang & Epstein, 1983). (Color figure can be viewed at wileyonlinelibrary.com)

56.3 and 57.7 wt% (Alexander et al., 2007). If we assume all IOM is hosted in the matrix, that gives matrix-normalized IOM abundances for Semarkona and Bishunpur of 4.1 and 1.8 wt%, respectively. With H/C atomic ratios of 0.25–0.48 (Alexander et al., 2007), IOM would contribute a limited fraction of the bulk H inventory of Semarkona and Bishunpur. In summary, the sharp decrease of bulk D/H ratios with progressive metamorphism of UOCs indicates that the high D/H component(s) is very susceptible to thermal alteration. Therefore, this D-rich material is likely inherited from the molecular cloud and/or disk processes, rather than being a product of secondary parent body processes. What this D/H-rich phase is remains to be firmly identified via in situ studies.

The high bulk δD value of 422‰ measured in Tieschitz (H/L3.6) is an outlier from the trend of decreasing D/H with increasing subtype. Tieschitz is an unusual chondrite, which exhibits unique properties relative to other UOCs. It contains two distinct matrix lithologies: a fine-grained so-called "black" matrix commonly forming a distinct component around chondrules, which contains an abundance of FeO-rich olivine (Alexander et al., 1989; Dobrică & Brearley, 2014), and "white" vein-like areas of matrix enriched in Na, Al, K and containing feldspars (e.g., Dobrică & Brearley, 2014). There is strong evidence that Tieschitz underwent hydrothermal alteration on its parent body, such as the presence of amphiboles in the black matrix (Dobrică & Brearley, 2014), despite the relatively low bulk water abundance of 0.29 wt% that we measured (Table 1). In addition, it has been suggested that the formation of the white matrix is due to interaction with a hydrous fluid on the parent body (Dobrică & Brearley, 2014; Hutchison et al., 1998). In situ studies of Tieschitz matrix would help decipher what phase(s) is responsible for its relatively high bulk D/H.

D/H Variation Across the Solar System

Our comprehensive D/H data set for bulk UOCs is compared to D/H values of a range of Solar System objects in Figure 7. The bulk Earth has a D/H ratio of ~155 × 10^{-6}, and the ice and gas giants have lower D/H ratios extending down to the D/H ratio of solar H_2 (Feuchtgruber et al., 2013; Geiss & Gloeckler, 2003; Mahaffy et al., 1998). Jupiter and Saturn are composed predominantly of H_2 gas and have D/H ratios similar to the protosolar nebula. In contrast, Neptune and Uranus are expected to have formed by additionally accreting icy, deuterium-rich planetesimals—such as comets—to construct their icy cores, thus giving them slightly higher D/H ratios relative to the protosolar nebula and gas giants.

The high bulk D/H ratios measured in UOCs (Figure 7), which originate from asteroidal bodies formed in the inner Solar System, do not readily conform to current models aimed at explaining the H isotope distribution and evolution in the early Solar System, despite these ratios likely being of a primary origin. Indeed, these models predict that the Solar System formed from a molecular cloud that contained D-

19455100, 2023, 9, Downloaded from https://onlinelibrary.wiley.com/doi/10.1111/maps.14041 by NICE, National Institute for Health and Care Excellence, Wiley Online Library on [16/10/2026]. See the Terms and Conditions (https://onlinelibrary.wiley.com/terms-and-conditions) on Wiley Online Library for rules of use; OA articles are governed by the applicable Creative Commons License

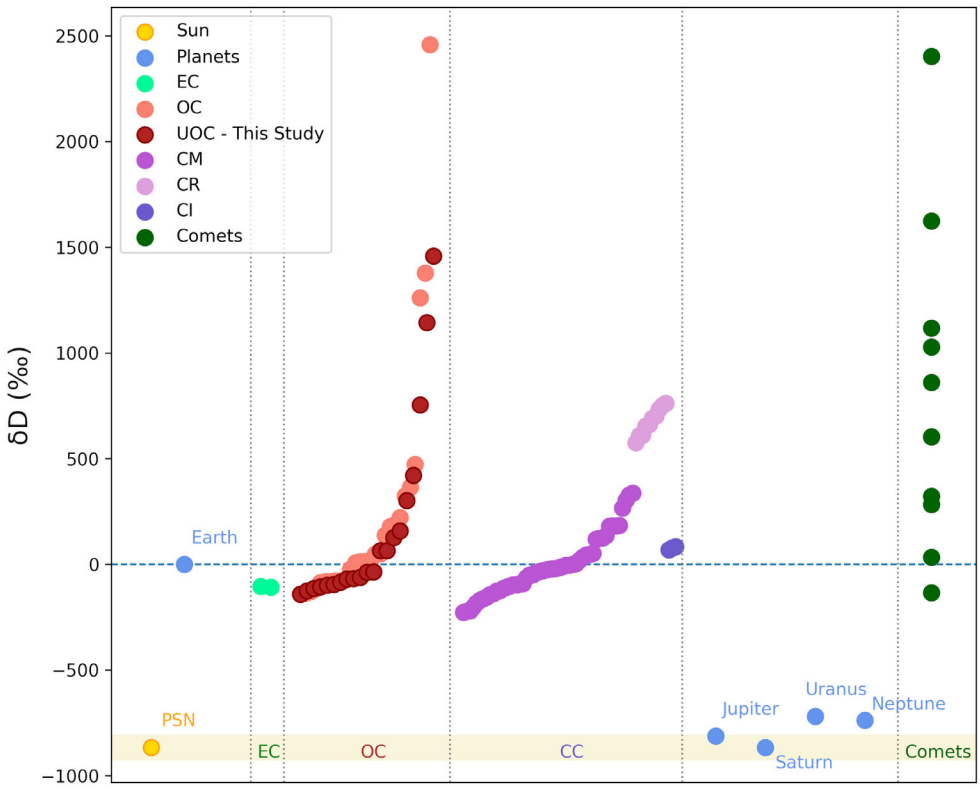

FIGURE 7. D/H ratios of a range of Solar System objects. Literature data are from McNaughton et al. (1981), McNaughton et al. (1982), Yang and Epstein (1983), Robert et al. (1987), Lécuyer et al. (1998), Lellouch et al. (2001), Geiss and Gloeckler (2003), Alexander et al. (2012), Feuchtgruber et al. (2013), Piani et al. (2020), Vacher et al. (2020), and references therein. The *x*-axis arbitrarily represents the order of distance from the Sun, and within chondrite groups, measurements are plotted in order of increasing D/H for simplicity. This is not intended to imply an increase in D/H based on distance from the Sun within a given chondrite group or class. (Color figure can be viewed at wileyonlinelibrary.com)

enriched water ice. Some of this D-rich water vaporized and underwent rapid isotopic exchange with D-depleted H_2 molecules in the warm (approximately 600–800 K) inner Solar System. Some of this D-depleted water was subsequently transported outward by turbulence, and recondensed outside the snowline into ice grains, which could then have been incorporated into small Solar System bodies. Therefore, there were at least two carriers of water in the early Solar System, pristine D-rich ice grains and D-poor condensed water vapor. To a first order, mixing between these D-poor and D-rich carriers resulted in water D/H approximately increasing with heliocentric distance from the Sun (e.g., Alexander et al., 2012; Drouart et al., 1999; Jacquet & Robert, 2013; Yang et al., 2013). The parent bodies of OCs are thought to have formed closer to the Sun than the parent bodies of volatile-rich CCs such as CR, CM, and CI chondrites (Alexander et al., 2018; Broadley et al., 2022; Scott et al., 2018; Trigo-Rodríguez et al., 2019). One would then expect the D/H ratio of the water accreted by the OC parent bodies to be lower than that of water accreted by those asteroidal bodies which formed further out in the Solar System. The bulk H isotope composition of the least metamorphosed UOCs shows that this is not the case, with D/H ratios of some of the most pristine UOCs being higher than the highest bulk CC D/H (Figure 7). This suggests that either UOC parent bodies accreted larger amounts of D-rich ices than CC parent bodies, or that carriers of these D-rich signatures were more efficiently altered and/or destroyed in CC.

A number of potential mechanisms may explain the observation that the least equilibrated UOCs have higher bulk D/H ratios than CCs. The most pristine UOC samples, such as Semarkona, have undergone very little alteration—thermal or aqueous—compared with the majority of CCs. Carbonaceous chondrite parent bodies may have accreted UOC-like D-rich ices, but these original signatures could have been lowered during fluid–rock interactions, resulting in lower D/H ratios such as those measured in water-rich CM and CI chondrites, for example. This is, however, unlikely as water in all CM chondrites displays similar D/H ratios, regardless of the degree of alteration (Piani et al., 2021; Piani & Marrocchi, 2018). In fact, the opposite isotopic

19455100, 2023, 9, Downloaded from https://onlinelibrary.wiley.com/doi/10.1111/maps.14041 by NICE, National Institute for Health and Care Excellence, Wiley Online Library on [16/10/2026]. See the Terms and Conditions (https://onlinelibrary.wiley.com/terms-and-conditions) on Wiley Online Library for rules of use; OA articles are governed by the applicable Creative Commons License

characteristics (i.e., low D/H with low metamorphism) would be expected if H-isotopic exchange between D-rich organic components and D-poor aqueous fluids were the dominant processes controlling D/H variations. In addition, other processes such as the aqueous oxidation of iron-bearing phases followed by H_2 loss and Rayleigh-type isotopic fractionation are likely ineffective for enriching D in water-rich chondrites, due to the buffering by large amounts of water. For CM chondrites, for example, this proposed mechanism is at odds with the observation that the least-altered CMs Paris and Asuka 12236 contain unoxidized metal and are enriched in D compared to more altered CMs (Marrocchi et al., 2023). Altogether, this suggests that the D-rich isotopic compositions of pristine UOCs are inherited characteristics involving processes having occurred in molecular cloud and/or protosolar nebula settings.

Observations and modeling of protoplanetary disks suggest that filaments (i.e., streamers) from the residual molecular clouds could inject D-rich material to the inner Solar System throughout the lifetime of the disk (Kuznetsova et al., 2022; Piani et al., 2021; Pineda et al., 2020). Provided this anisotropic (unidirectional) infall has a precise enough deposition throughout its lifetime (i.e., injecting into small enough regions to only affect a singular population of disk material—the OCs), and that it could transport sufficient D-enriched material, this could help explain the anomalously high D/H ratios observed in UOCs compared to CCs, without having to reassess existing models for the spatial and temporal evolution of the water H isotope composition in the early Solar System. This process also offers the advantage of producing a complex, unequilibrated mixture of organics and water ice grains bearing large and variable H isotopic variations.

CONCLUSION

This mineralogical and geochemical study of a comprehensive set of unequilibrated ordinary chondrites shows that the least metamorphosed fall samples contain up to 1 wt% H_2O, associated with very high bulk δD values of up to 1500‰. These bulk water abundances are consistent with the presence of an XRD amorphous component, which likely includes matrix phyllosilicates. Bulk D/H ratios in UOCs decrease rapidly with increasing levels of metamorphism, indicating that the high D/H host(s) is sensitive to thermal alteration. In situ analyses in matrix areas of Semarkona (Piani et al., 2015), coupled with the limited abundance of insoluble organic matter in the most pristine UOCs (Alexander et al., 2007), indicate that this high D/H component is not organic. Precisely identifying this high D/H component, and why D/H ratios decline sharply with progressive metamorphism, will require further in situ investigations on a range of petrologic subtypes.

The most pristine unequilibrated ordinary chondrites such as Semarkona and Bishunpur have some of the highest bulk D/H ratios in the Solar System, much higher than D/H of other inner Solar System objects and volatile-rich carbonaceous chondrites. This is particularly enigmatic when considering that OC parent bodies formed closer to the Sun than CC parent bodies, thus not conforming to the expected D/H increase with heliocentric distance. This may indicate localized deposition of D-rich filaments from the molecular cloud and/or outer Solar System in the OC parent body forming region, which CC parent bodies would have escaped. Alternatively, both OC and CC parent bodies may have originally accreted this D-rich component, which would have been subsequently altered in water-rich CC parent bodies due to extensive hydrothermal alteration.

Acknowledgments—We thank the UK Science and Technology Facilities Council (grants ST/P005225/1 to R. T.; ST/V000675/1 to R. J.; and a studentship ST/T50628X/1 to H. G.), UK Research and Innovation (grant MR/T020261/1 to A. K.), and the Agence Nationale de la Recherche (grant ANR-19-CE31-0027-01 HYDRaTE to L.P.) for funding. We also thank François Robert and Timothy Jull for their constructive suggestions, Jens Najorka for help with the XRD setup, and the Natural History Museum (London), the American Museum of Natural History (NYC), the Smithsonian Institution (Washington, DC), and CEREGE (Aix-en-Provence) for loans of the studied samples.

Data Availability Statement—The data that supports the findings of this study are available in the supplementary material of this article.

Editorial Handling—Dr. A. J. Timothy Jull

REFERENCES

Alexander, C. M. O'D., Bowden, R., Fogel, M. L., Howard, K. T., Herd, C. D. K., and Nittler, L. R. 2012. The Provenances of Asteroids, and their Contributions to the Volatile Inventories of the Terrestrial Planets. *Science* 337: 721–3.

Alexander, C. M. O'D., Fogel, M., Yabuta, H., and Cody, G. D. 2007. The Origin and Evolution of Chondrites Recorded in the Elemental and Isotopic Compositions of their Macromolecular Organic Matter. *Geochimica et Cosmochimica Acta* 71: 4380–403. https://doi.org/10.1016/j.gca.2007.06.052.

Alexander, C. M. O'D., Howard, K. T., Bowden, R., and Fogel, M. L. 2013. The Classification of CM and CR Chondrites Using Bulk H, C and N Abundances and

19455100, 2023, 9, Downloaded from https://onlinelibrary.wiley.com/doi/10.1111/maps.14041 by NICE, National Institute for Health and Care Excellence, Wiley Online Library on [16/10/2026]. See the Terms and Conditions (https://onlinelibrary.wiley.com/terms-and-conditions) on Wiley Online Library for rules of use; OA articles are governed by the applicable Creative Commons License

Isotopic Compositions. *Geochimica et Cosmochimica Acta* 123: 244–60. https://doi.org/10.1016/j.gca.2013.05.019.

Alexander, C. M. O'D., Hutchison, R., and Barber, D. J. 1989. Origin of Chondrule Rims and Interchondrule Matrices in Unequilibrated Ordinary Chondrites. *Earth & Planetary Science Letters* 95: 187–207. https://doi.org/10.1016/j.gca.2010.05.005.

Alexander, C. M. O'D., McKeegan, K. D., and Altwegg, K. 2018. Water Reservoirs in Small Planetary Bodies: Meteorites, Asteroids, and Comets. *Space Science Reviews* 214: 36. https://doi.org/10.1007/s11214-018-0474-9.

Alexander, C. M. O'D., Newsome, S. D., Fogel, M. L., Nittler, L. R., Busemann, H., and Cody, G. D. 2010. Deuterium Enrichments in Chondritic Macromolecular Material—Implications for the Origin and Evolution of Organics, Water and Asteroids. *Geochimica et Cosmochimica Acta* 74: 4417–37. https://doi.org/10.1016/j.gca.2010.05.005.

Batchelder, M., and Cressey, G. 1998. Rapid, Accurate Phase Quantification of Clay-Bearing Samples Using a Position-Sensitive X-Ray Detector. *Clays & Clay Minerals* 46: 183–94.

Bland, P. A., Cressey, G., and Menzies, O. 2004. Modal Mineralogy of Carbonaceous Chondrites by X-Ray Diffraction and Mössbauer Spectroscopy. *Meteoritics & Planetary Science* 39: 3–16. https://doi.org/10.2307/j.ctv1v7zdmm.

Bonal, L., Quiric, E., and Bourot-Denise, M. 2004. Petrologic Type of CV3 Chondrites as Revealed by Raman Spectroscopy of Organic Matter. *35th Lunar and Planetary Science Conference*, abstract #1562.

Brearley, A., and Jones, R. H. 1998. Chondritic Meteorites. In *Planetary Materials*, edited by J. J. Papika, 191–244. Washington, DC: Mineralogical Society of America. https://doi.org/10.1515/9781501508806-018.

Broadley, M., Bekaert, D., Piani, L., Füri, E., and Marty, B. 2022. Origin of Life-Forming Volatile Elements in the Inner Solar System. *Nature* 611: 245–55. https://doi.org/10.1038/s41586-022-05276-x.

Busemann, H., Young, A. F., Alexander, C. M. O'D., Hoppe, P., Mukhopadhyay, S., and Nittler, L. R. 2006. Interstellar Chemistry Recorded in Organic Matter from Primitive Meteorites. *Science* 312: 727–30. https://doi.org/10.1126/science.1123878.

Ceccarelli, C., Caselli, P., Bockelee-Morvan, D., Mousis, O., Pizzarello, S., Robert, F., and Semenov, D. 2014. Deuterium Fractionation: The Ariadne's Thread from the Pre-Collapse Phase to Meteorites and Comets Today. In *Protostars and Planets VI*, edited by H. Beuther, R. S. Klessen, C. P. Dullemond, and T. Henning, 859–83. Tucson, AZ: University of Arizona Press. https://doi.org/10.2458/azu_uapress_9780816531240-ch037.

Choi, B.-G., McKeegan, K. D., Krot, A. N., and Wasson, J. T. 1998. Extreme Oxygen-Isotope Compositions in Magnetite from Unequilibrated Ordinary Chondrites. *Nature* 392: 577–9. https://doi.org/10.1038/33356.

Deloule, E., and Robert, F. 1995. Interstellar Water in Meteorites? *Geochimica et Cosmochimica Acta* 59: 4695–706. https://doi.org/10.1016/0016-7037(95)00313-4.

Desch, S. J., Kalyaan, A., and Alexander, C. M. O'D. 2018. The Effect of Jupiter's Formation on the Distribution of Refractory Elements and Inclusions in Meteorites. *The Astrophysical Journal Supplement Series* 238: 11. https://doi.org/10.3847/1538-4365/aad95f.

Dobrică, E., and Brearley, A. J. 2014. Widespread Hydrothermal Alteration Minerals in the Fine-Grained Matrices of the Tieschitz Unequilibrated Ordinary Chondrite. *Meteoritics & Planetary Science* 49: 1323–49. https://doi.org/10.1111/maps.12335.

Dobrică, E., and Brearley, A. J. 2020. Amorphous Silicates in the Matrix of Semarkona: The First Evidence for the Localized Preservation of Pristine Matrix Materials in the most Unequilibrated Ordinary Chondrites. *Meteoritics & Planetary Science* 55: 649–68. https://doi.org/10.1111/maps.13458.

Dobrică, E., Le Guillou, C., and Brearley, A. J. 2019. Aqueous Alteration of Porous Microchondrules in Semarkona: Implications for Hydration, Oxidation and Elemental Exchange Processes. *Geochimica et Cosmochimica Acta* 244: 292–307. https://doi.org/10.1016/j.gca.2018.10.002.

Drouart, A., Dubrulle, B., Gautier, D., and Robert, F. 1999. Structure and Transport in the Solar Nebula from Constraints on Deuterium Enrichment and Giant Planets Formation. *Icarus* 140: 129–55. https://doi.org/10.1006/icar.1999.6137.

Dunn, T. L., Cressey, G., McSween, H. Y. Jr, and McCoy, T. J. 2010. Analysis of Ordinary Chondrites Using Powder X-ray Diffraction: 1. Modal Mineral Abundances. *Meteoritics & Planetary Science* 45: 123–34. https://doi.org/10.1111/j.1945-5100.2009.01011.x

Feuchtgruber, H., Lellouch, E., Orton, G., de Graauw, T., Vandenbussche, B., Swinyard, B., Moreno, R., et al. 2013. The D/H Ratio in the Atmospheres of Uranus and Neptune from Herschel-PACS Observations. *Astronomy & Astrophysics* 551: A126. https://doi.org/10.1051/0004-6361/201220857.

Gaffey, M. J., and Gilbert, S. L. 1998. Asteroid 6 Hebe: The Probable Parent Body of the H-Type Ordinary Chondrites and the IIE Iron Meteorites. *Meteoritics & Planetary Science* 33: 1281–95. https://doi.org/10.1111/j.1945-5100.1998.tb01312.x.

Geiss, J., and Gloeckler, G. 2003. Isotopic Composition of H, HE and NE in the Protosolar Cloud. *Space Seviews* 106: 3–18. https://doi.org/10.1023/A:1024651232758.

Grossman, J. N., Alexander, C. M. O'D., Wang, J., and Brearley, A. J. 2000. Bleached Chondrules: Evidence for Widespread Aqueous Processes on the Parent Asteroids of Ordinary Chondrites. *Meteoritics & Planetary Science* 35: 467–86. https://doi.org/10.1111/j.1945-5100.2000.tb01429.x.

Grossman, J. N., and Brearley, A. J. 2005. The Onset of Metamorphism in Ordinary and Carbonaceous Chondrites. *Meteoritics & Planetary Science* 40: 87–122. https://doi.org/10.1111/j.1945-5100.2005.tb00366.x.

Hallis, L. J. 2017. D/H Ratios of the Inner Solar System. *Philosophical Transactions. Series A: Mathematical, Physical, and Engineering Sciences* 375: 20150390. https://doi.org/10.1098/rsta.2015.0390.

Hallis, L. J., Huss, G. R., Nagashima, K., Taylor, G. J., Halldórsson, S. A., Hilton, D. R., Mottl, M. J., and Meech, K. J. 2015. Evidence for Primordial Water in Earth's Deep Mantle. *Science* 350: 795–7. https://doi.org/10.1126/science.aac4834.

Howard, K. T., Benedix, G. K., Bland, P. A., and Cressey, G. 2009. Modal Mineralogy of CM2 Chondrites by X-Ray Diffraction (PSD-XRD). Part 1: Total Phyllosilicate Abundance and the Degree of Aqueous Alteration. *Geochimica et Cosmochimica Acta* 73: 4576–89. https://doi.org/10.1016/j.gca.2009.04.038.

Huss, G. R., Keil, K., and Taylor, G. J. 1981. The Matrices of Unequilibrated Ordinary Chondrites: Implications for

19455100, 2023, 9, Downloaded from https://onlinelibrary.wiley.com/doi/10.1111/maps.14041 by NICE, National Institute for Health and Care Excellence, Wiley Online Library on [16/10/2026]. See the Terms and Conditions (https://onlinelibrary.wiley.com/terms-and-conditions) on Wiley Online Library for rules of use; OA articles are governed by the applicable Creative Commons License

the Origin and History of Chondrites. *Geochimica et Cosmochimica Acta* 45: 33–51. https://doi.org/10.1016/0016-7037(81)90262-3.

Huss, G. R., Rubin, A. E., and Grossman, J. N. 2006. Thermal Metamorphism in Chondrites. 2006. In *Meteorites and the Early Solar System II*, edited by D. S. Lauretta, and H. Y. McSween, 567–86. Tucson, AZ: University of Arizona Press. https://ui.adsabs.harvard.edu/abs/2006mess.book..567H.

Hutchison, R., Alexander, C. M. O'D., and Barber, D. J. 1987. The Semarkona Meteorite: First Recorded Occurrence of Smectite in an Ordinary Chondrite, and its Implications. *Geochimica et Cosmochimica Acta* 51: 1875–82. https://doi.org/10.1016/0016-7037(87)90178-5.

Hutchison, R., Alexander, C. M. O'D., and Bridges, J. C. 1998. Elemental Redistribution in Tieschitz and the Origin of White Matrix. *Meteoritics & Planetary Science* 33: 1169–79. https://doi.org/10.1111/j.1945-5100.1998.tb01721.x.

Ito, M., Tomioka, N., Uesugi, M., Yamaguchi, A., Shirai, N., Ohigashi, T., Liu, M. C., et al. 2022. A Pristine Record of Outer Solar System Materials from Asteroid Ryugu's Returned Sample. *Nature Astronomy* 6: 1163–71. https://doi.org/10.1038/s41550-022-01745-5.

Jacquet, E., and Robert, F. 2013. Water Transport in Protoplanetary Disks and the Hydrogen Isotopic Composition of Chondrites. *Icarus* 223: 722–32. https://doi.org/10.1016/j.icarus.2013.01.022.

King, A. J., Schofield, P. F., Howard, K. T., and Russell, S. S. 2015. Modal Mineralogy of CI and CI-Like Chondrites by X-Ray Diffraction. *Geochimica et Cosmochimica Acta* 165: 148–60. https://doi.org/10.1016/j.gca.2015.05.038.

Kleine, T., Budde, G., Burkhardt, C., Kruijer, T. S., Worsham, E. A., Morbidelli, A., and Nimmo, F. 2020. The Non-Carbonaceous–Carbonaceous Meteorite Dichotomy. *Space Science Reviews* 216: 27–55. https://doi.org/10.1007/s11214-020-00675-w.

Krot, A. N., Doyle, P. M., Nagashima, K., Dobrică, E., and Petaev, M. I. 2022. Mineralogy, Petrology, and Oxygen-Isotope Compositions of Magnetite ± Fayalite Assemblages in CO3, CV3, and LL3 Chondrites. *Meteoritics & Planetary Science* 57: 392–428. https://doi.org/10.1111/maps.13709.

Krot, A. N., Hutcheon, I. D., Brearley, A. J., Pravdivtseva, O. V., Petaev, M. I., and Hohenberg, C. M. 2006. Timescales and Settings for Alteration of Chondritic Meteorites. In *Meteorites and the Early Solar System II*, edited by D. S. Lauretta, and H. Y. McSween, 525–53. Tucson, AZ: University of Arizona Press.

Krot, A. N., and Rubin, A. E. 1994. Glass-Rich Chondrules in Ordinary Chondrites. *Meteoritics* 29: 697–707. https://doi.org/10.1111/j.1945-5100.1994.tb00787.x.

Krot, A. N., Scott, E. R. D., and Zolensky, M. E. 1997. Origin of Fayalitic Olivine Rims and Lath-Shaped Matrix Olivine in the CV3 Chondrite Allende and its Dark Inclusions. *Meteoritics & Planetary Science* 32: 31–49. https://doi.org/10.1111/j.1945-5100.1997.tb01238.x.

Kruijer, T. S., Burkhardt, C., Budde, G., and Kleine, T. 2017. Age of Jupiter Inferred from the Distinct Genetics and Formation Times of Meteorites. *Proceedings of the National Academy of Sciences of the United States of America* 114: 6712–6. https://doi.org/10.1073/pnas.1704461114.

Kuznetsova, A., Bae, J., Hartmann, L., and Mac Low, M.-M. 2022. Anisotropic Infall and Substructure Formation in Embedded Disks. *The Astrophysical Journal* 928: 92–109. https://doi.org/10.3847/1538-4357/ac54a8.

Lécuyer, C., Gillet, P., and Robert, F. 1998. The Hydrogen Isotope Composition of Seawater and the Global Water Cycle. *Chemical Geology* 145: 249–61. https://doi.org/10.1016/S0009-2541(97)00146-0.

Lellouch, E., Bézard, B., Fouchet, T., Feuchtgruber, H., Encrenaz, T., and de Graauw, T. 2001. The Deuterium Abundance in Jupiter and Saturn from ISO-SWS Observations. *Astronomy & Astrophysics* 370: 610–22. https://doi.org/10.1051/0004-6361:20010259.

Lewis, J. A., and Jones, R. H. 2019. Primary Feldspar in the Semarkona LL3.00 Chondrite: Constraints on Chondrule Formation and Secondary Alteration. *Meteoritics & Planetary Science* 54: 72–89. https://doi.org/10.1111/maps.13194.

Lewis, J. A., Jones, R. H., and Brearley, A. J. 2022. Plagioclase Alteration and Equilibration in Ordinary Chondrites: Metasomatism during Thermal Metamorphism. *Geochimica et Cosmochimica Acta* 316: 201–29. https://doi.org/10.1016/j.gca.2021.10.004.

Lichtenberg, T., Drążkowska, J., Schönbächler, M., Golabek, G. J., and Hands, T. O. 2021. Bifurcation of Planetary Building Blocks during Solar System Formation. *Science* 371: 365–70. https://doi.org/10.1126/science.abb3091.

Mahaffy, P. R., Donahue, T. M., Atreya, S. K., Owen, T. C., and Niemann, H. B. 1998. Galileo Probe Measurements of D/H and 3He/4He in Jupiter's Atmosphere. *Space Science Reviews* 84: 251–63. https://doi.org/10.1023/A:1005091806594.

Marrocchi, Y., Bonal, L., Gattacceca, J., Piani, L., Beck, P., Greenwood, R., Eschrig, J., Basque, A., Nuccio, P. M., and Martin, F. F. 2020. The Piancaldoli Meteorite: A Forgotten Primitive LL3.10 Ordinary Chondrite. *Meteoritics & Planetary Science* 55: 1924–35. https://doi.org/10.1111/maps.13552.

Marrocchi, Y., Rigaudier, T., Piralla, M., and Piani, L. 2023. Hydrogen Isotopic Evidence for Nebular Pre-Hydration and the Limited Role of Parent-Body Processes in CM Chondrites. *Earth & Planetary Science Letters* 611: 118151. https://doi.org/10.1016/j.epsl.2023.118151.

McNaughton, N. J., Borthwick, J., Fallick, A. E., and Pillinger, C. T. 1981. Deuterium/Hydrogen Ratios in Unequilibrated Ordinary Chondrites. *Nature* 294: 639–41. https://doi.org/10.1038/294639a0.

McNaughton, N. J., Borthwick, J., Fallick, A. E., and Pillinger, C. T. 1982. Deuterium Enrichments in Primitive Meteorites. *Journal of Geophysical Research: Solid Earth* 87(S01): A297–302.

Menzies, O. N., Bland, P. A., Berry, F. J., and Cressey, G. 2005. A Mössbauer Spectroscopy and X-Ray Diffraction Study of Ordinary Chondrites: Quantification of Modal Mineralogy and Implications for Redox Conditions during Metamorphism. *Meteoritics & Planetary Science* 40: 1023–42.

Müller, D. R., Altwegg, K., Berthelier, J. J., Combi, M., De Keyser, J., Fuselier, S. A., Hänni, N., et al. 2022. High D/H Ratios in Water and Alkanes in Comet 67P/Churyumov-Gerasimenko Measured with Rosetta/ROSINA DFMS. *Astronomy & Astrophysics* 662: A69. https://doi.org/10.1051/0004-6361/202142922.

Piani, L., and Marrocchi, Y. 2018. Hydrogen Isotopic Composition of Water in CV-Type Carbonaceous Chondrites. *Earth & Planetary Science Letters* 504: 64–71. https://doi.org/10.1016/j.epsl.2018.09.031.

Piani, L., Marrocchi, Y., Rigaudier, T., Vacher, L. G., Thomassin, D., and Marty, B. 2020. Earth's Water may

19455100, 2023, 9, Downloaded from https://onlinelibrary.wiley.com/doi/10.1111/maps.14041 by NICE, National Institute for Health and Care Excellence, Wiley Online Library on [16/10/2026]. See the Terms and Conditions (https://onlinelibrary.wiley.com/terms-and-conditions) on Wiley Online Library for rules of use; OA articles are governed by the applicable Creative Commons License

have been Inherited from Material Similar to Enstatite Chondrite Meteorites. *Science* 369: 1110–3. https://doi.org/10.1126/science.aba1948.

Piani, L., Marrocchi, Y., Vacher, L. G., Yurimoto, H., and Bizzarro, M. 2021. Origin of Hydrogen Isotopic Variations in Chondritic Water and Organics. *Earth & Planetary Science Letters* 567: 117008. https://doi.org/10.1016/j.epsl.2021.117008.

Piani, L., Robert, F., and Remusat, L. 2015. Micron-Scale D/H Heterogeneity in Chondrite Matrices: A Signature of the Pristine Solar System Water? *Earth & Planetary Science Letters* 415: 154–64. https://doi.org/10.1016/j.epsl.2015.01.039.

Pineda, J. E., Segura-Cox, D., Caselli, P., Cunningham, N., Zhao, B., Schmiedeke, A., Maureira, M. J., and Neri, R. 2020. A Protostellar System Fed by a Streamer of 10,500 au Length. *Nature Astronomy* 4: 1158–63. https://doi.org/10.1038/s41550-020-1150-z.

Remusat, L., Piani, L., and Bernard, S. 2016. Thermal Recalcitrance of the Organic D-Rich Component of Ordinary Chondrites. *Earth & Planetary Science Letters* 435: 36–44. https://doi.org/10.1016/j.epsl.2015.12.009.

Robert, F. 2006. Solar System Deuterium/Hydrogen Ratio. In *Meteorites and the Early Solar System II*, edited by D. S. Lauretta, and H. Y. McSween, 341–51. Tucson, AZ: University of Arizona Press.

Robert, F., Derenne, S., Lombardi, G., Hassouni, K., Michau, A., Reinhardt, P., Duhamel, R., Gonzale, A., and Biron, K. 2017. Hydrogen Isotope Fractionation in Methane Plasma. *Proceedings of the National Academy of Sciences of the United States of America* 114: 870–4. https://doi.org/10.1073/pnas.1615767114.

Robert, F., Javoy, M., Halbout, J., Dimon, B., and Merlivat, L. 1987. Hydrogen Isotope Abundances in the Solar System. Part I: Unequilibrated Chondrites. *Geochimica et Cosmochimica Acta* 51: 1787–805. https://doi.org/10.1016/0016-7037(87)90170-0.

Robert, F., Merlivat, L., and Javoy, M. 1979. Deuterium Concentration in the Early Solar System: Hydrogen and Oxygen Isotope Study. *Nature* 282: 785–9. https://doi.org/10.1038/282785a0.

Rubin, A. E., Trigo-Rodríguez, J. M., Huber, H., and Wasson, J. T. 2007. Progressive Aqueous Alteration of CM Carbonaceous Chondrites. *Geochimica et Cosmochimica Acta* 71: 2361–82. https://doi.org/10.1016/j.gca.2007.02.008.

Schofield, P. F., Knight, K. S., Covey-Crump, S. J., Cressey, G., and Stretton, I. C. 2002. Accurate Quantification of the Modal Mineralogy of Rocks when Image Analysis is Difficult. *Mineralogical Magazine* 66: 189–200. https://doi.org/10.1180/0026461026610022.

Scott, E. R. D., Krot, A. N., and Sanders, I. S. 2018. Isotopic Dichotomy among Meteorites and its Bearing on the Protoplanetary Disk. *The Astrophysical Journal* 854: 164–76. https://doi.org/10.3847/1538-4357/aaa5a5.

Sears, D. W. G., Hasan, F. A., Batchelor, J. D., and Lu, J. 1991. Chemical and Physical Studies of Type 3 Chondrites—XI: Metamorphism, Pairing, and Brecciation of Ordinary Chondrites. *Lunar and Planetary Science Conference Proceedings* 21: 493–512.

Sears, D. W. G., Morse, A. D., Hutchison, R., Guimon, R. K., Jie, L., Alexander, C. M. O'D., Benoit, P. H., et al. 1995. Metamorphism and Aqueous Alteration in Low Petrographic Type Ordinary Chondrites. *Meteoritics* 30: 169–81. https://doi.org/10.1111/j.1945-5100.1995.tb01112.x.

Semenenko, V. P., Bischoff, A., Weber, I., Perron, C., and Girich, A. L. 2001. Mineralogy of Fine-Grained Material in the Krymka (LL3.1) Chondrite. *Meteoritics & Planetary Science* 36: 1067–86. https://doi.org/10.1111/j.1945-5100.2001.tb01945.x.

Semenenko, V. P., Jessberger, E. K., Chaussidon, M., Weber, I., Stephan, T., and Wies, C. 2005. Carbonaceous Xenoliths in the Krymka LL3.1 Chondrite: Mysteries and Established Facts. *Geochimica et Cosmochimica Acta* 69: 2165–82. https://doi.org/10.1016/j.gca.2004.10.027.

Trigo-Rodríguez, J. M., Rimola, A., Tanbakouei, S., Soto, V. C., and Lee, M. 2019. Accretion of Water in Carbonaceous Chondrites: Current Evidence and Implications for the Delivery of Water to Early Earth. *Space Science Reviews* 215: 18–27. https://doi.org/10.1007/s11214-019-0583-0.

Vacher, L. G., Piani, L., Rigaudier, T., Thomassin, D., Florin, G., Piralla, M., and Marrocchi, Y. 2020. Hydrogen in Chondrites: Influence of Parent Body Alteration and Atmospheric Contamination on Primordial Components. *Geochimica et Cosmochimica Acta* 281: 53–66. https://doi.org/10.1016/j.gca.2020.05.007.

Velbel, M. A., and Zolensky, M. E. 2021. Thermal Metamorphism of CM Chondrites: A Dehydroxylation-Based Peak-Temperature Thermometer and Implications for Sample Return from Asteroids Ryugu and Bennu. *Meteoritics & Planetary Science* 56: 546–85. https://doi.org/10.1111/maps.13636.

Vernazza, P., Zanda, B., Nakamura, T., Scott, E., and Russell, S. S. 2015. The Formation and Evolution of Ordinary Chondrite Parent Bodies. In *Asteroids IV*, edited by P. Michel, F. E. DeMeo, and W. F. Bottke, 617–34. Tucson, AZ: University of Arizona Press. https://doi.org/10.2458/azu_uapress_9780816532131-ch032.

Warren, P. H. 2011a. Stable-Isotopic Anomalies and the Accretionary Assemblage of the Earth and Mars: A Subordinate Role for Carbonaceous Chondrites. *Earth & Planetary Science Letters* 311: 93–100. https://doi.org/10.1016/j.epsl.2011.08.047.

Warren, P. H. 2011b. Stable Isotopes and the Noncarbonaceous Derivation of Ureilites, in Common with Nearly All Differentiated Planetary Materials. *Geochimica et Cosmochimica Acta* 75: 6912–26. https://doi.org/10.1016/j.gca.2011.09.011.

Weisberg, M. K., McCoy, T. J., and Krot, A. N. 2006. Systematics and Evaluation of Meteorite Classification. In *Meteorites and the Early Solar System II*, edited by D. S. Lauretta, and H. Y. McSween, 19–52. Tucson, AZ: University of Arizona Press. https://doi.org/10.2307/j.ctv1v7zdmm.

Weisberg, M. K., Zolensky, M. E., and Prinz, M. 1997. Fayalitic Olivine in Matrix of the Krymka LL3.1 Chondrite: Vapor-Solid Growth in the Solar Nebula. *Meteoritics & Planetary Science* 32: 791–801. https://doi.org/10.1111/j.1945-5100.1997.tb01570.x.

Wolters, F., and Emmerich, K. 2007. Thermal Reactions of Smectites—Relation of Dehydroxylation Temperature to Octahedral Structure. *Thermochimica Acta* 462: 80–8. https://doi.org/10.1016/j.tca.2007.06.002.

Wood, J. A. 1962. Metamorphism in Chondrites. *Geochimica et Cosmochimica Acta* 26: 739–49. https://doi.org/10.1016/0016-7037(62)90036-4.

Yang, J., and Epstein, S. 1983. Interstellar Organic Matter in Meteorites. *Geochimica et Cosmochimica Acta* 47: 2199–216. https://doi.org/10.1016/0016-7037(83)90043-1.

19455100, 2023, 9, Downloaded from https://onlinelibrary.wiley.com/doi/10.1111/maps.14041 by NICE, National Institute for Health and Care Excellence, Wiley Online Library on [16/10/2026]. See the Terms and Conditions (https://onlinelibrary.wiley.com/terms-and-conditions) on Wiley Online Library for rules of use; OA articles are governed by the applicable Creative Commons License

Yang, L., Ciesla, F. J., and Alexander, C. M. O'D. 2013. The D/H Ratio of Water in the Solar Nebula during its Formation and Evolution. *Icarus* 226: 256–67. https://doi.org/10.1016/j.icarus.2013.05.027.

Yoshikawa, M., Fujiwara, A., Kawaguchi, J., and Hayabusa Mission and Science Team. 2007. The Nature of Asteroid Itokawa Revealed by Hayabusa. *Proceedings of the International Astronomical Union* 2: 401–16. https://doi.org/10.1017/S174392130700350X.

SUPPORTING INFORMATION

Additional supporting information may be found in the online version of this article.

Figure S1. Bulk mineral abundances determined from high flux XRD analyses. UOCs are ordered from left to right in order of increasing petrologic subtype.

Table S1. Bulk mineral abundances determined from high flux XRD, where olivine compositions are given in increments of 20% and pyroxene is divided into enstatite and augite.

Data S1. Bulk IRMS data of D/H ratios and H_2O contents, including standards.

Data S2. Raw XRD spectra.

19455100, 2023, 9, Downloaded from https://onlinelibrary.wiley.com/doi/10.1111/maps.14041 by NICE, National Institute for Health and Care Excellence, Wiley Online Library on [16/10/2026]. See the Terms and Conditions (https://onlinelibrary.wiley.com/terms-and-conditions) on Wiley Online Library for rules of use; OA articles are governed by the applicable Creative Commons License